

Applications of Isothermal Titration Calorimetry in Protein Folding and Molecular Recognition

Y. Liang

State Key Laboratory of Virology, College of Life Sciences, Wuhan University, Wuhan 430072, China

(Received 3 May 2006, Accepted 18 June 2006)

During the past decade, isothermal titration calorimetry (ITC) has developed from a specialist method to a major, commercially available tool in the arsenal directed at understanding molecular interactions. At present, ITC is used to study all types of binding reactions, including protein-protein, protein-ligand, DNA-drug, DNA-protein, receptor-target, and enzyme kinetics, and it is becoming the method of choice for the determination of the thermodynamic parameters associated with the structure transformation of one molecule or non-covalent interaction of two (or more) molecules. Here, the new applications of ITC in protein folding/unfolding and misfolding, as well as its traditional application in molecular interaction/recognition are reviewed, providing an overview of what can be achieved in these fields using this method and what developments are likely to occur in the near future.

Keywords: Isothermal titration calorimetry, Protein folding/unfolding and misfolding, Molecular interaction/recognition

INTRODUCTION

Isothermal titration calorimetry (ITC), which provides a direct route to the complete thermodynamic characterization of non-covalent, equilibrium interactions, has become the fastest developing technique in biological research [1-3] since its emergence in the field of scientific research in 1989. In ITC, a syringe containing a "ligand" is titrated into a cell containing a solution of the "macromolecule". As the two elements interact, heat is released or absorbed in direct proportion to the amount of binding that occurs. When the macromolecule in the cell becomes saturated with added ligand, the heat signal diminishes until only the background heat of dilution is observed. Measurement of this heat allows for the very accurate determination of binding constants (K_B), reaction stoichiometry (n), and a thermodynamic profile of the reaction

that includes the observed molar calorimetric enthalpy (ΔH_{obs}), entropy (ΔS_{obs}), heat capacity ($\Delta C_{p,\text{obs}}$) of binding and change in free energy (ΔG). Unlike other methods, ITC does not require immobilization and/or modification of reactants since heat of binding is a naturally occurring phenomenon [1-4].

During the past decade the number of those proficient in this field has multiplied dramatically. This has led to an overwhelming amount of new data and novel applications of ITC to be assessed. The complete thermodynamic characterization of a bimolecular interaction can be determined in a simple experiment resulting in the generation of a large amount of data in a short time. Some reasons for the increasing popularity of ITC are: (1) the experiment is relatively easy to perform; (2) although an absolute thermodynamic quantification of a particular event is difficult to ascertain, there are methods to deconvolve various terms; (3) in some instances, the K_B values of a series of interactions are similar or indistinguishable [5], however, the determination of

*Corresponding author. E-mail: liangyi@whu.edu.cn

the ΔH and ΔS terms allows a further level of discrimination; (4) although it is not possible to provide a full thermodynamic-structure correlation from an ITC experiment, it is possible to draw sensible conclusions from data by comparing systems where subtle changes have been imposed; (5) the correlation of the ΔC_p term with the change in surface area buried on the formation of a bimolecular interface has proven to be a useful tool in understanding the structure and thermodynamics of interactions [6,7]. ITC experiments performed at different temperatures provide an accurate and direct determination of the ΔC_p term. It should be pointed out that this correlation should come with a warning that it can be misleading in some cases [1]. Nevertheless, the widespread commercial availability of isothermal titration calorimeters has revolutionized the study of biochemistry and biophysics. The recent development of high-sensitivity instruments allowing rapid, accurate thermodynamic characterization of binding events has provided a new level of information which will help to better understand the mechanisms of biomolecular interactions [1-4].

At present, ITC is used to study all types of binding reactions, including protein-protein, protein-ligand [4], DNA-drug, DNA-protein, receptor-target, and enzyme kinetics, and it is becoming the method of choice for the determination of the thermodynamic parameters associated with the structure transformation of one molecule or non-covalent interaction of two (or more) molecules. In this review, the new applications of ITC in protein folding/unfolding and misfolding as well as its traditional application in molecular interaction/recognition are discussed, providing an overview of what can be achieved in these fields using this method and what developments are likely to occur in the near future.

ITC APPLICATIONS IN PROTEIN FOLDING/UNFOLDING AND MISFOLDING

Although the mechanisms of these phenomena have been widely discussed since the pioneering studies of Anfinsen, knowledge about the thermodynamics of protein folding/unfolding and misfolding is relatively limited. ITC is a powerful tool for the study of both thermodynamic and kinetic properties of protein folding by virtue of its general applicability and high precision, yielding some useful

thermodynamic data on protein folding/unfolding and misfolding [8-13].

In a publication from my laboratory, the unfolding of bovine liver catalase induced by guanidine hydrochloride (GuHCl) has been studied by ITC [8]. At 25.0 °C, the measurements of intrinsic enthalpy, Gibbs free energy, and entropy changes for the formation of the partially folded activated dimer of this protein in the presence of low GuHCl concentrations were found to be $-69.2 \text{ kJ mol}^{-1}$, 6.43 kJ mol^{-1} and $-254 \text{ J K}^{-1} \text{ mol}^{-1}$, respectively. The stabilization and activation of this partially folded dimer by GuHCl originate from the entropic and electrostatic effects of this denaturant [8]. ITC was further employed in the study of the unfolding of rabbit muscle creatine kinase (MM-CK) induced by acid [9]. The results indicate that the unfolding of MM-CK induced by acid is driven by a favorable enthalpy change, with an unfavorable entropy decrease at lower temperature (15.0 °C), becoming entropy-driven at higher temperatures (25.0, 30.0, and 37.0 °C). The increase in $\Delta_{\text{conf}}H_m$ with increasing temperature at pH 3.5 or 4.0 indicates that thermal unfolding occurs. The changes in enthalpy and entropy for the unfolding strongly depend on temperature, whereas the Gibbs free energy change of the unfolding is almost temperature-independent. The enthalpy change for the unfolding is almost compensated for by a corresponding change in entropy, resulting in a smaller net Gibbs free energy increase. That is, remarkable enthalpy-entropy compensation occurs in the unfolding of the protein induced by acid, suggesting that water reorganization is involved in the unfolding reaction. The value of $\Delta_U G_m^\circ$ for the unfolding of MM-CK induced by GuHCl ($6.24 \text{ kcal mol}^{-1}$) [10] is two-fold of that induced by acid ($3.37 \text{ kcal mol}^{-1}$) [9], indicating that the degree of protein unfolding when induced by acid is less than that induced by guanidine hydrochloride [10].

Isothermal acid-titration calorimetry (IATC) is a new method for evaluating the pH dependence of protein enthalpy. In a recent publication by Nakamura and Kidokoro [11], the enthalpy change accompanying the reversible acid-induced transition from the native (N) to the molten-globule (MG) state of bovine cytochrome c has been directly evaluated by this method. The results of the global analysis of the temperature dependence of the excess enthalpy from 20 to 35 °C have demonstrated that the N to MG transition is a two-

state transition with a small heat capacity change.

We have studied the thermodynamics of the refolding of denatured D-glyceraldehyde 3-phosphate dehydrogenase (GAPDH) assisted by protein disulfide isomerase (PDI), a molecular chaperone, using ITC at different molar ratios of PDI/GAPDH and temperatures using two thermodynamic models proposed for chaperone-substrate binding and chaperone-assisted substrate folding, respectively [12]. The binding of GAPDH folding intermediates to PDI is driven by a large favorable enthalpy decrease with a large unfavorable entropy reduction, and shows strong enthalpy-entropy compensation and weak temperature dependence of Gibbs free energy change. A large negative heat-capacity change of binding indicates that hydrophobic interaction is a major force for the binding. The binding stoichiometry shows one dimeric GAPDH intermediate per PDI monomer. The refolding of GAPDH assisted by PDI is a largely exothermic reaction at 15.0-25.0 °C. With an increase in temperature from 15.0 to 37.0 °C, the PDI-assisted reactivation yield of denatured GAPDH decreases upon dilution. However, at 37.0 °C, the spontaneous reactivation, PDI-assisted reactivation and intrinsic molar enthalpy change during the PDI-assisted refolding of GAPDH were not detected at all [12].

Protein misfolding and aggregation are interconnected processes involved in a wide variety of nonneuropathic, systemic, and neurodegenerative diseases, including Alzheimer's, Parkinson's, and prion diseases. Kardos *et al.* [13] have reported for the first time a direct thermodynamic study of amyloid formation using ITC. β_2 -Microglobulin, a protein responsible for dialysis-related amyloidosis, has been used for extending amyloid fibrils in a seed-controlled reaction in the cell of the calorimeter. The enthalpy and heat capacity changes of the reaction have been investigated, where the monomeric, acid-denatured molecules adopt an ordered, cross- β -sheet structure in the rigid amyloid fibrils. Despite the dramatic difference in morphology, β_2 -microglobulin has exhibited a similar heat capacity change upon amyloid formation to that seen when folding into the native globular state, whereas the enthalpy change of the reaction has proven to be markedly lower. In comparison with the native state, the results outline the important structural features of the amyloid fibrils: a similar extent of surface burial even with the supramolecular architecture of amyloid fibrils, a lower level of internal

packing, and the possible presence of unfavorable side chain contributions [13].

We have studied the oxidative refolding of reduced, denatured hen egg-white lysozyme in the presence of a mixed macromolecular crowding agent containing both bovine serum albumin and polysaccharide from a physiological point of view [14]. Both the refolding yield and the rate of the oxidative refolding of lysozyme in these mixed crowded solutions with suitable weight ratios are higher than those in single crowded solutions, indicating that mixed macromolecular crowding agents are more favorable to lysozyme folding and can be used to simulate intracellular environments more accurately than single crowding agents. Meanwhile, we have investigated the molar enthalpy changes accompanying the refolding of lysozyme in the presence of mixed macromolecular crowding agents using ITC. Figure 1 compares the ITC curves of the refolding of reduced, denatured lysozyme in the refolding buffer with a mixed macromolecular crowding agent (10 g l⁻¹ BSA + 90 g l⁻¹ dextran 70), and without macromolecular crowding agents. As shown in Fig. 1, the apparent enthalpy change is negative at the first titration of reduced, denatured lysozyme to the refolding buffer, and then it increases gradually to zero in the presence of mixed macromolecular crowding agents, while it increases gradually to a positive value in the absence of macromolecular crowding agents. Figure 2 shows the average value of the apparent molar enthalpy change accompanying the refolding of lysozyme in the presence of mixed or single macromolecular crowding agents. It can be seen from Fig. 2 that the apparent molar enthalpy change in the presence of crowding agents is negative and very large, except for dextran 70, while that in the absence of crowding agents is positive and very small. These results indicate that the thermodynamic behavior of a protein during its refolding in a crowded environment is absolutely different from that under dilute experimental conditions.

PROTEIN-PROTEIN INTERACTIONS

Protein-protein interactions (PPIs) play key roles in many essential biological processes, such as the assembly of cellular components, the conveyance by transport machinery across the various biological membranes, signal transduction, and the

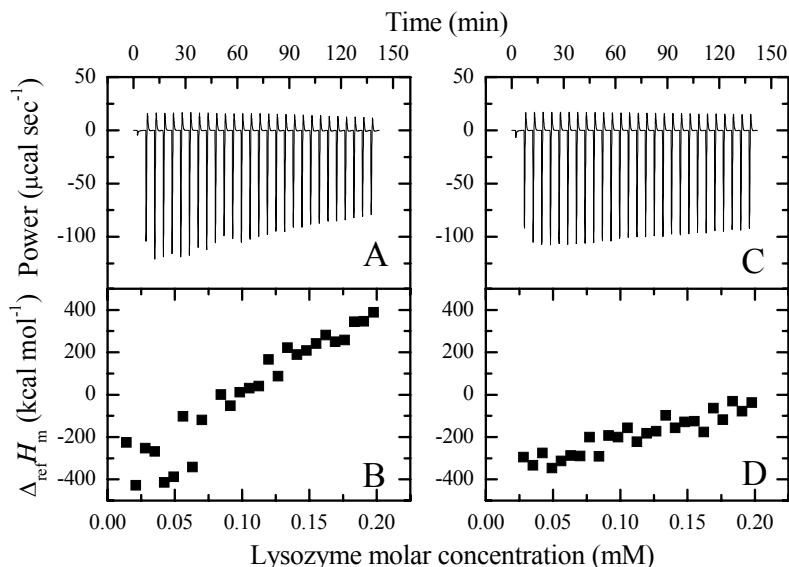


Fig. 1. ITC curves and apparent molar enthalpy changes during reduced, denatured lysozyme titrated to the refolding buffer in the absence of crowding agents (A and B) and in the presence of 100 g l⁻¹ mixed crowding agent (10 g l⁻¹ BSA + 90 g l⁻¹ dextran 70) (C and D).

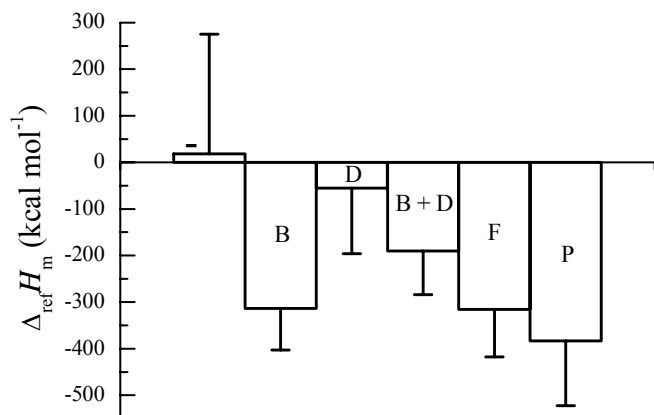


Fig. 2. The intrinsic molar enthalpy change for the refolding of reduced, denatured lysozyme in the refolding buffer in the absence of crowding agents (-) and in the presence of 100 g l⁻¹ BSA (B), 100 g l⁻¹ dextran 70 (D), 100 g l⁻¹ Ficoll 70 (F), 100 g l⁻¹ PEG (P) and a mixed crowding agent containing 10 g l⁻¹ BSA + 90 g l⁻¹ dextran 70 (B + D). Each bar represents the average value of the apparent molar enthalpy changes accompanying titration repeated 28 times. Errors shown are the standard errors of the mean.

regulation of gene expression and enzymatic activities [15]. ITC is the most quantitative means available for measuring the thermodynamic properties of protein-protein interactions and is becoming a necessary tool for PPI complex structural studies [1-3,15-24].

Xanthine oxidase (XO) and copper, zinc superoxide dismutase (Cu,Zn-SOD) are function-related proteins *in vivo*. We have studied the thermodynamics of the interaction of bovine milk XO with bovine erythrocyte Cu,Zn-SOD using ITC [15]. The binding of XO to Cu,Zn-SOD is driven by a large favorable enthalpy decrease with a large unfavorable entropy reduction, and shows strong entropy-enthalpy compensation and weak temperature-dependence of Gibbs free energy change. An unexpected, large positive molar heat capacity change of the binding, 3.02 kJ mol⁻¹ K⁻¹, at all temperatures examined suggests that either hydrogen bonding or long-range electrostatic interaction is a major force for the binding. However, the large unfavorable change in entropy suggests that long-range electrostatic forces do not play an important role in the binding. These results indicate that XO binds to Cu,Zn-SOD with high affinity and that hydrogen bonding is a major force for the binding [15].

Lukasik and co-workers [18] have explained how the C-

terminal coiled-coil domain from smooth muscle myosin heavy chain (CBF β -SMMHC) fusion protein can perturb > 50% of normal Runx1-CBF β function using the results from ITC, and demonstrated that the CBF β -SMMHC protein binds to the Runt domain from Runx1 with both higher affinity and altered stoichiometry relative to the native CBF β . Their data, which reveal how CBF β -SMMHC inactivate the majority of the Runx1 protein in the cell, also clearly suggest that targeting of the CBF β -SMMHC protein for drug development may be a viable approach to the treatment of certain leukemias. This higher affinity provides an explanation for the dominant negative phenotype associated with a knock-in of the CBF β -MYH11 gene, and helps to provide a rationale for the leukemia-associated dysregulation of hematopoietic development that this protein causes.

Glycoprotein folding and quality control in the endoplasmic reticulum (ER) are assisted by two homologous molecular chaperones, calreticulin (CRT) and the membrane-bound calnexin (CNX). CRT and CNX are lectins that interact with ERp57, a thiol-disulfide oxidoreductase that promotes the formation of disulfide bonds in glycoproteins bound by CRT. During the folding of viral glycoproteins in the ER of living cells, ERp57 has been shown to form transient intermolecular disulfide bonds with glycoprotein substrates bound to CNX and CRT [19]. To gain insights into the cooperation of CRT and CNX with ERp57 during glycoprotein folding, Frickel *et al.* [20] have characterized the interaction between the CRT P-domain and ERp57 by using ITC. Their results have shown that the dissociation constant of the CRT (189-288)/ERp57 complex is $(9.1 \pm 3.0) \times 10^{-6}$ M at 8 °C. Combined with the results from NMR, they have analyzed the functional mechanism of the CRT/ERp57 chaperone system [20].

The Golgi-associated, γ -adaptin-related, ADP-ribosylation-factor binding proteins (GGAs) and adaptor protein (AP)-1 are adaptors involved in clathrin-mediated transport between the *trans*-Golgi network and the endosomal system. The appendage domains of GGAs and the AP-1 γ -adaptin subunit are structurally homologous and have been proposed to bind to accessory proteins *via* interaction with short sequences containing phenylalanines and acidic residues. Collins and colleagues [21] have presented the structure of the human GGA1 appendage in complex with its cognate binding peptide from the p56 accessory protein (DDDDFGGFEEAETFD) as

determined by X-ray crystallography. The interaction is governed predominantly by the packing of the first two phenylalanine residues of the peptide with conserved basic and hydrophobic residues from GGA1. Additionally, several main chain hydrogen bonds cause the peptide to form an additional β -strand on the edge of the preexisting β -sheet of the protein. So they have used ITC to assess the affinities of different peptides for the GGA and γ -appendage domains. These types of interactions are necessary for establishing the dynamic networks of components that mediate complex cellular activities such as transport-vesicle biogenesis and regulation [21].

The association of two proteins can be described as a two-step process, with the formation of an encounter complex followed by desolvation and establishment of a tight complex. Kiel and co-workers [22] have designed a set of mutants of the Ras effector protein Ral guanine nucleotide dissociation stimulator (RalGDS) with optimized electrostatic steering. The results from ITC and other biophysical methods have shown that the fastest binding RalGDS mutants, M26K, D47K and E54K, bind Ras 14-fold faster and 25-fold tighter than the wild type. Upon further formation of the final complex, the increased Coulombic interactions are probably counterbalanced by the cost of desolvation of charges, keeping the dissociation rate constant almost unchanged. This mechanism is also reflected by the mutual compensation of enthalpy and entropy changes quantified by ITC. The binding constants of the faster binding RalGDS mutants toward Ras are similar to those of Raf, the most prominent Ras effector, suggesting that the design methodology may be used to switch between signal transduction pathways [22].

ATP hydrolysis by the Hsp90 molecular chaperone requires a connected set of conformational switches triggered by ATP binding to the N-terminal domain in the Hsp90 dimer. Hsp90 mutants that influence these conformational switches have strong effects on ATPase activity. ATPase activity is specifically regulated by Hsp90 co-chaperones, which directly influence the conformational switches. Siligardi and colleagues [23] have analyzed the effect of Hsp90 mutations on the binding and ATPase regulation by the co-chaperones, Aha1, Sti1 and Sba1, using ITC and other biophysical methods. The ability of Sti1 to bind Hsp90 and arrest its ATPase activity is not affected by any of the mutants screened.

In the presence of the ATP analogue adenylyl-5'-yl imidodiphosphate (AMPPNP), Sba1 binds to wild-type and ATPase hyperactive mutants with similar affinity, but only very weakly to hypoactive mutants despite their wild-type ATP affinity. Unexpectedly, in all cases, Sba1 binds to Hsp90 with a 1:2 molar stoichiometry. Analysis of complex formation with co-chaperone mixtures has shown that Aha1 and p50^{cdc37} are able to bind Hsp90 simultaneously, but without direct interaction. Sba1 and p50^{cdc37} bind independently to Hsp90-AMPPNP but not together. This shows that, by influencing the conformational state of the “ATP lid” and consequent N-terminal dimerization, Sba1 and Aha1 regulate Hsp90, but Sti1 does not [23].

Elucidation of the roles of the hydrogen bonds involved in antigen-antibody complementary association requires both structural and thermodynamic information. Yokota and co-workers [24] have examined the interaction between hen egg-white lysozyme (HEL) and its HyHEL-10 variable domain fragment (Fv) antibody. They have constructed three antibody mutants and investigated the interactions between the mutant Fvs and HEL. The results from ITC have indicated that the mutations significantly decreased the negative enthalpy change, despite some offset by a favorable entropy change. X-ray crystallography has demonstrated that the complexes had nearly identical structures, including the positions of the interfacial water molecules. Taken together, the ITC and X-ray crystallographic results indicate that hydrogen bonding *via* interfacial water enthalpically contributes to the Fv-HEL interaction despite the partial offset because of entropy loss, suggesting that hydrogen bonding stiffens the antigen-antibody complex [24].

PROTEIN-SMALL MOLECULE INTERACTIONS

The interactions of proteins with small molecules are of much importance to biology. An understanding of the molecular basis of protein-small molecule interactions is crucial to attempts to design novel drug technologies. The thermodynamic information of the protein-small molecule interactions obtained from ITC [25-32] facilitates the understanding of the binding modes, and is helpful to the development of novel drugs for some serious diseases.

We have investigated the interactions between *Trichoderma reesei* cellulase and an anionic surfactant, sodium dodecyl sulfate (SDS), at critical micelle concentration using ITC and other biophysical methods [25]. SDS micelles have dual interactions with cellulase: first electrostatic and then hydrophobic interactions. When the concentration of SDS is lower than 45.0 mM, SDS micelles cause a partial loss in the hydrolytic activity together with a steep decrease in the α -helical content of cellulase. By increasing the concentration of SDS, however, a reformation of the α -helical structure and a partial recovery of the hydrolytic activity of cellulase induced by SDS micelles are observed. Taken together, our results indicate that, through binding, SDS micelles exert a dual effect on cellulase as both a denaturant and a recovery reagent.

Bicyclomycin, a hexameric helicase essential to many bacteria, terminates nascent RNA transcripts utilizing ATP hydrolysis, and is the only natural product inhibitor of the transcription termination factor rho with weak binding affinity. Using ITC, Brogan *et al.* [26] have found that the designed bicyclomycin ligand, 5a-(3-formyl-phenylsulfanyl)-dihydro-bicyclomycin, inhibits rho an order of magnitude more efficiently than bicyclomycin [26].

Sawas and co-workers [27] have directly examined the enthalpic contributions to binding of closely related anesthetic haloethers (desflurane, isoflurane, enflurane, and sevoflurane) and halothane to bovine and human serum albumin (BSA and HSA) in aqueous solution using ITC. The binding of these anesthetic compounds to serum albumin is exothermic, yielding enthalpies of -3 to -6 kcal mol⁻¹ for BSA with a rank order of apparent equilibrium association constants of desflurane > isoflurane ~ enflurane > halothane \geq sevoflurane, with the differences being largely ascribed to entropic contributions. The magnitude of the observed ΔH increased linearly with an increase in temperature, reflecting negative changes in heat capacities. From these results, they have inferred that solvent restructuring, resulting from the release of water weakly bound to anesthetic and anesthetic-binding sites, is a dominant and favorable contributor to the enthalpy and entropy of binding to proteins [27].

Garnier *et al.* [28] have studied the interactions of ATP with native Hsp90 and its recombinant N-terminal and C-terminal domains by ITC. Their results have clearly demonstrated that Hsp90 possesses a second ATP-binding site

located on the C-terminus of the protein. The binding constant between this domain of Hsp90 and ATP-Mg and a comparison with the binding constant on the full-length protein are reported. It is proposed that this potential Rossmann fold may constitute the C-terminal ATP-binding site [28].

Thompsett and colleagues [29] have used ITC to determine the affinity of copper for wild type mouse PrP protein and a series of mutants. High affinity copper binding by wild type PrP has been confirmed, indicating the presence of specific tight copper binding sites with up to femtomolar affinity. Altogether, four high affinity binding sites with between femto- and nanomolar affinities are located within the octameric repeat region of the protein at physiological pH. A fifth copper binding site of lower affinity than those of the octameric repeat region has been detected in full-length protein [29].

Bingham and co-workers [30] have examined the thermodynamics of binding of two related pyrazine-derived ligands to the major urinary protein, MUP-I. Global thermodynamics data derived from ITC indicate that binding is driven by favorable enthalpic contributions, rather than the classical entropy-driven hydrophobic effect. Unfavorable entropic contributions from the protein backbone and side-chain residues in the vicinity of the binding pocket are partially offset by favorable entropic contributions at adjacent positions, suggesting a “conformational relay” mechanism whereby increased rigidity of residues on ligand binding is accompanied by increased conformational freedom of side chains in adjacent positions.

HasA_{SM} secreted by the Gram-negative bacterium *Serratia marcescens* belongs to the hemophore family. Its role is to take up heme from host heme carriers and to shuttle it to specific receptors. Heme is linked to the HasA_{SM} protein by the unusual axial ligand pair, His32 and Tyr75. The nucleophilic nature of the tyrosine is enhanced by the hydrogen bonding of the tyrosinate to the neighboring histidine in the binding site, His83. Deniau *et al.* [31] have used ITC to examine the thermodynamics of heme binding to HasA_{SM} and have shown that this binding is strongly exothermic and enthalpy driven. They have also analyzed the thermodynamics of the interaction between heme and a panel of single, double, and triple mutants of the two axial ligands His32 and Tyr75 and of His83 to assess the implication of

each of these three residues in heme binding. They have demonstrated that, in contrast to His32, His83 is essential for the binding of heme to HasA_{SM}, even though it is not directly coordinated to iron, and that the Tyr75/His83 pair plays a key role in the interaction [31].

Expression of brain fatty acid-binding protein is spatially and temporally correlated with neuronal differentiation during brain development. ITC has been used to demonstrate that recombinant human brain fatty acid-binding protein clearly exhibits high affinity for unsaturated fatty acids, such as oleic acid, but has low binding affinity for saturated long chain fatty acids [32]. The three-dimensional structure of this protein in complex with oleic acid shows that the oleic acid hydrocarbon tail assumes a “U-shaped” conformation, whereas in the complex with docosahexaenoic acid the hydrocarbon tail adopts a helical conformation. Furthermore, analysis of the primary and tertiary structures of this protein provides a rationale for its high affinity and specificity for unsaturated fatty acids [32].

NUCLEIC ACID-SMALL MOLECULE INTERACTIONS

During the past decade, the interaction of small molecules, including metal complexes, with DNA and RNA has attracted much attention, and the use of these complexes as probes of the structures of DNA and RNA sites has proven to be quite fruitful [33,34]. Recently, ITC has yielded some useful thermodynamic data on small molecule-RNA/DNA interactions [33-39]. Information obtained from ITC will be helpful to the understanding of the mechanism of the interactions of small molecules with nucleic acids, and should be useful in the development of nucleic acid molecular probes and new therapeutic reagents for some diseases related to viruses such as AIDS and SARS.

We have used ITC and other biophysical tools to conduct thermodynamic and kinetic investigations of the scission of calf thymus DNA (CT DNA) catalyzed by bleomycin A₅ (BLM-A₅) in the presence of ferrous ions and oxygen [33]. The catalytic efficiency of BLM-A₅ is of the same order of magnitude as that of lysozyme, but several orders of magnitude lower than those of *TaqI* restriction endonuclease, *NaeI* endonuclease and *BamHI* endonuclease. By comparing

the molar enthalpy change for the cleavage of CT DNA induced by BLM-A₅ with that of the scission of CT DNA mediated by adriamycin and by (1,10-phenanthroline)-copper, it was found that BLM-A₅ possessed the highest DNA cleavage efficiency among these DNA-damaging agents. Our results suggest that BLM-A₅ is not as efficient as a DNA-cleaving enzyme, although the cleavage of DNA by BLM-A₅ follows Michaelis-Menten kinetics. Binding of BLM-A₅ to CT DNA is driven by a favorable entropy increase with a less favorable enthalpy decrease, in line with a partial intercalation mode involved in BLM-catalyzed breakage of DNA.

We have employed ITC and other biophysical methods to investigate the interactions of a metal complex [Ru(phen)₂PMIP]²⁺ {Ru = ruthenium, phen = 1,10-phenanthroline, PMIP = 2-(4-methylphenyl)imidazo[4,5-f]1,10-phenanthroline} with yeast tRNA and CT DNA [34]. Spectroscopic studies together with ITC and viscosity measurements indicate that both binding modes of the Ru(II) polypyridyl complex to yeast tRNA and CT DNA are intercalation and yeast tRNA binding of the complex is stronger than CT DNA binding. ITC experiments show that the interaction of the complex with yeast tRNA is driven by a moderately favorable enthalpy decrease in combination with a moderately favorable entropy increase, while the binding of the complex to CT DNA is driven by a large favorable enthalpy decrease with a less favorable entropy increase. The results from equilibrium dialysis and CD suggest that both interactions are enantioselective and the Δ enantiomer of the complex may bind more favorably to both yeast tRNA and CT DNA than the Λ enantiomer, and that the complex is a better candidate for an enantioselective binder to yeast tRNA than to CT DNA. Taken together, our results indicate that the structures of nucleic acids have significant effects on the binding behaviors of metal complexes.

Barceló and colleagues [35] have used ITC and other biophysical tools to analyze the multivalent (intercalation plus minor groove) binding of the antitumor antibiotic chartreusin to DNA, and have obtained a detailed thermodynamic profile for the interaction of this multivalent drug. Their results indicate that the main contributor to the free energy of binding is the hydrophobic transfer of the chartreusin chromophore from the solution to the DNA intercalating site.

Hutchins and co-workers [36] have investigated the DNA

binding energetics of a series of analogues derived from the anticancer agent N-[2-(dimethylamino)ethyl]-9-amino-acridine-4-carboxamide (AAC). ITC and spectrophotometry have been used to determine the effects of substituent modification at the C5 position of the acridine chromophore on the interaction of AAC with DNA. Energetic profiles describing ligand-DNA complex formation obtained from ITC indicate that C5 substitution significantly enhances binding enthalpy relative to the parent AAC. In many cases, the enhanced binding enthalpies of the C5-substituted analogues correlate with anticancer activity.

Qu *et al.* [37] have investigated the thermodynamic binding of the intercalator 7-amino actinomycin D to DNA using ITC. They have indicated that the flanking sequences not only affect DNA stability and secondary structure, but also modulate ligand binding to the primary binding site. The magnitude of the ligand binding affinity to the primary site is inversely related to the sequence dependent stability. Their results have revealed a pronounced enthalpy-entropy compensation for 7-amino actinomycin D binding to this family of oligonucleotides and have suggested that the DNA sequences flanking the primary binding site can strongly influence ligand recognition of specific sites on target DNA molecules [37].

Lah and Vesnaver [38] have studied the energetics of interactions occurring in the model ligand-DNA systems constituted from distamycin A, netropsin, and oligomeric duplexes using ITC and other biophysical tools. Their results have revealed several unprecedented ligand-DNA binding features. The hydrophobic transfer of ligand from the solution into the duplex binding site, and the accompanying specific non-covalent ligand-DNA interactions, occur within the DNA minor groove.

Aluminum is a known neurotoxic agent and its neurotoxic effects may be due to its binding to DNA. However, the mechanism for the interaction of aluminum ions with DNA is not well understood. We have used ITC and other biophysical methods to investigate the thermodynamics of the binding of aluminum ions to CT DNA under various pH and temperature conditions [39]. Figure 3A shows the ITC curve of the interaction of aluminum ions with CT DNA at 37.0 °C in ammonium acetate buffer at pH 4.0. Fig. 3B displays a plot of the heat evolved per mole of aluminum ions added, corrected

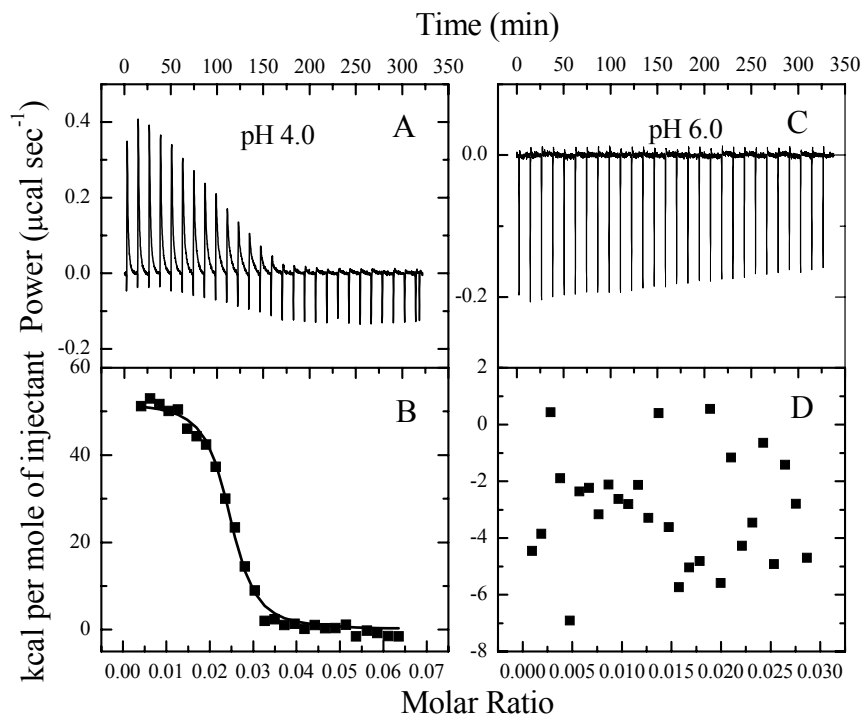


Fig. 3. ITC measurements of the binding of aluminum ions to CT DNA at 37.0 °C in 0.1 M ammonium acetate buffer at pH 4.0 and 6.0. (A) Typical calorimetric titration of CT DNA (300 μ M) with aluminum ions (88.7 μ M) at pH 4.0. (B) Plot of the heat evolved (kcal) per mole of aluminum ions added, corrected for the heat of aluminum dilution, against the molar ratio of aluminum ions to CT DNA at pH 4.0. The data (solid squares) were fitted to a single set of identical sites model and the solid line represented the best fit. (C) Typical calorimetric titration of CT DNA (300 μ M) with aluminum ions (40.0 μ M) at pH 6.0. (D) Plot of the heat evolved (kcal) per mole of aluminum ions added, corrected for the heat of aluminum dilution, against the molar ratio of aluminum ions to CT DNA at pH 6.0. The data (solid squares) were too small to be fitted, indicating that no binding was observed under these conditions.

for the heat of aluminum dilution, against the molar ratio of aluminum ions to CT DNA at pH 4.0. The binding reaction is driven entirely by a large favorable entropy increase, accompanied by an unfavorable enthalpy increase in the pH range of 3.5-5.5 at all temperatures examined. Aluminum ions show a strong pH-dependent binding affinity to CT DNA. A large positive molar heat capacity change for the binding demonstrates the burial of the polar surface of CT DNA upon groove binding. The binding constant increases with the increase in pH, reaching a maximum at pH 4.5, thereafter declining as the pH increases further, up to 5.5. Figure 3C shows the ITC curve of the interaction of aluminum ions with

CT DNA at 37.0 °C in ammonium acetate buffer at pH 6.0. Fig. 3D displays a plot of the heat evolved per mole of aluminum ions added, corrected for the heat of aluminum dilution, against the molar ratio of aluminum ions to CT DNA at pH 6.0. At pH 6.0 and 7.0, aluminum ions precipitate CT DNA completely and no binding of aluminum ions to CT DNA is observed by ITC. Combining the results from these methods, we conclude that aluminum ions bind to CT DNA with high affinity through groove binding under aluminum toxicity pH conditions and precipitate CT DNA under physiological conditions [39]. These thermodynamic findings have provided further insights into the mechanism by which

aluminum functions as both a groove binder and a precipitating agent, and help to explain the role of this metal in the pathogenesis of Alzheimer's disease and other human brain disorders.

CONCLUSIONS

The ITC method is gaining wider usage in the investigation of molecular interaction/recognition, and deeper usage with respect to the investigation of protein folding/unfolding and misfolding. The proliferation of this method in academic and industrial laboratories has produced many new reports of interesting applications, new systems studied, and advances in data analysis. By analyzing the experimental data from new applications of ITC in protein folding/unfolding and misfolding, as well as its traditional application in molecular interaction/recognition, scientists will improve their understanding of the relationships between the ITC data and structural details. To ensure the effectiveness of ITC results, advancements in the analysis of ITC need to be achieved. Thus, to understand the complexities of protein folding and molecular recognition, scientists must combine X-ray crystallography and NMR spectroscopy with ITC.

ACKNOWLEDGEMENTS

The following financial support is gratefully acknowledged: National Natural Science Foundation of China Grants 30370309 and 90408012, Project 863 Grant 2004AA404260 from the Ministry of Science and Technology of China, and the Program for New Century Excellent Talents in University Grant NCET-04-0670 from the Ministry of Education of China.

REFERENCES

- [1] M.J. Cliff, A. Gutierrez, J.E. Ladbury, *J. Mol. Recognit.* 17 (2004) 513.
- [2] A. Ababou, J.E. Ladbury, *J. Mol. Recognit.* 19 (2006) 79.
- [3] M.J. Cliff, J.F. Ladbury, *J. Mol. Recognit.* 16 (2003) 383.
- [4] A.A. Saboury, *J. Iranian Chem. Soc.* 3 (2006) 1.
- [5] B.M. Baker, K.P. Murphy, *Biophys. J.* 71 (1996) 2049.
- [6] P.R. Connelly, R. Varadarajan, J.M. Sturtevant, F.M. Richards, *Biochemistry* 29 (1990) 6108.
- [7] R. Spolar, M.T. Record, *Science* 263 (1994) 777.
- [8] M. Jiao, Y. Liang, H.T. Li, X. Wang, *Acta. Chim. Sinica* 61 (2003) 1362.
- [9] Y. Liang, F. Du, S. Sanglier, B.R. Zhou, Y. Xia, A.V. Dorsseleer, C. Maechling, M.C. Kilhoffer, J. Haiech, *J. Biol. Chem.* 278 (2003) 30098.
- [10] Y.X. Fan, J.M. Zhou, H. Kihara, C.L. Tsou, *Protein Sci.* 7 (1998) 2631.
- [11] S. Nakamura, S. Kidokoro, *Biophys. Chem.* 113 (2005) 161.
- [12] Y. Liang, J. Li, J. Chen, C.C. Wang, *Eur. J. Biochem.* 268 (2001) 4183.
- [13] J. Kardos, K. Yamamoto, K. Hasegawa, H. Naiki, Y. Goto, *J. Biol. Chem.* 279 (2004) 55308.
- [14] B.R. Zhou, Y. Liang, F. Du, Z. Zhou, J. Chen, *J. Biol. Chem.* 279 (2004) 55109.
- [15] Y.L. Zhou, J.M. Liao, F. Du, Y. Liang, *Thermochim. Acta* 426 (2005) 173.
- [16] M.M. Pierce, C.S. Raman, B.T. Nall, *Methods* 19 (1999) 213.
- [17] W.E. Stites, *Chem. Rev.* 97 (1997) 1233.
- [18] S.M. Lukasik, L. Zhang, T. Corpora, S. Tomanicek, Y.H. Li, M. Kundu, K. Hartman, P.P. Liu, T.M. Laue, R.L. Biltonen, N.A. Speck, J.H. Bushweller, *Nature structural biology* 9 (2002) 674.
- [19] M. Molinari, A. Helenius, *Nature* 402 (1999) 90.
- [20] E.M. Frickel, R. Riek, I. Jelesarov, A. Helenius, K. Wüthrich, L. Ellgaard, *P. Natl. Acad. Sci. USA* 99 (2002) 1954.
- [21] B.M. Collins, G.J.K. Praefcke, M.S. Robinson, D.J. Owen, *Nature Structural Biology* 10 (2003) 607.
- [22] C. Kiel, T. Selzer, Y. Shaul, G. Schreiber, C. Herrmann, *P. Natl. Acad. Sci. USA* 101 (2004) 9223.
- [23] G. Siligardi, B. Hu, B. Panaretou, P.W. Piper, L.H. Pearl, C. Prodromou, *J. Biol. Chem.* 279 (2004) 51989.
- [24] A. Yokota, K. Tsumoto, M. Shiroishi, H. Kondo, I. Kumagai, *J. Biol. Chem.* 278 (2003) 5410.
- [25] J. Xiang, J.B. Fan, N. Chen, J. Chen, Y. Liang, *Colloids Surf. B: Biointerfaces* 49 (2006) 175.
- [26] A.P. Brogan, W.R. Widger, D. Bensadek, I. Riba-

Applications of isothermal titration calorimetry

- Garcia, S.J. Gaskell, H. Kohn, *J. Am. Chem. Soc.* 127 (2005) 2741.
- [27] A.H. Sawas, S.N. Pentyala, M.J. Rebecchi, *Biochemistry* 43 (2004) 12675.
- [28] C. Garnier, D. Lafitte, P.O. Tsvetkov, P. Barbier, J. Leclerc-Devin, J. Millot, C. Briand, A.A. Makarov, M.G. Catelli, V. Peyrot, *J. Biol. Chem.* 277 (2002) 12208.
- [29] A.R. Thompsett, S.R. Abdelraheim, M. Daniels, D.R. Brown, *J. Biol. Chem.* 280 (2005) 42750.
- [30] R.J. Bingham, J.B.C. Findlay, S. Hsieh, A.P. Kalverda, A. Kjellberg, C. Perazzolo, S.E.V. Phillips, K. Seshadri, C.H. Trinh, W.B. Turnbull, G. Bodenhausen, S.W. Homans, *J. Am. Chem. Soc.* 126 (2004) 1675.
- [31] C. Deniau, R. Gilli, N. Izadi-Pruneyre, S. Létoffé, M. Delepierre, C. Wandersman, C. Briand, A. Lecroisey, *Biochemistry* 42 (2003) 10627.
- [32] G.K. Balendiran, F. Schnütgen, G. Scapin, T. Borchers, N.g. Xhong, K. Lim, R. Godbout, F. Spener, J.C. Sacchettini, *J. Biol. Chem.* 275 (2000) 27045.
- [33] Y. Liang, F. Du, B.R. Zhou, H. Zhou, G.L. Zou, C.X. Wang, *Eur. J. Biochem.* 269 (2002) 2851.
- [34] H. Xu, Y. Liang, P. Zhang, F. Du, B.R. Zhou, J. Wu, J.H. Liu, Z.G. Liu, L.N. Ji, *J. Biol. Inorg. Chem.* 10 (2005) 529.
- [35] F. Barceló, D. Capó, J. Portugal, *Nucleic Acids Res.* 30 (2002) 4567.
- [36] R.A. Hutchins, J.M. Crenshaw, D.E. Graves, W.A. Denny, *Biochemistry* 42 (2003) 13754.
- [37] X.G. Qu, J.S. Ren, P.V. Riccelli, A.S. Benight, J.B. Chaires, *Biochemistry* 42 (2003) 11960.
- [38] J. Lah, G. Vesnaver, *J. Mol. Biol.* 342 (2004) 73.
- [39] J. Wu, F. Du, P. Zhang, I.A. Khan, J. Chen, Y. Liang, *J. Inorg. Biochem.* 99 (2005) 1145.